A Quantitative XANES Analysis of the Calcium High-Affinity Binding Site of the Purple Membrane

Francesc Sepulcre,* M. Grazia Proietti,† Maurizio Benfatto,‡ Stefano Della Longa,‡¶ Joaquin García,† and Esteve Padrós§

*Departament d'Enginyeria Agroalimentària i Biotecnologia, Escola Superior d'Agricultura, Universitat Politècnica de Catalunya, Barcelona, Spain; †Instituto de Ciencia de los Materiales de Aragón, CSIC-Universidad de Zaragoza, Facultad de Ciencias, Zaragoza, Spain; ‡Laboratori Nazionali di Frascati-INFN, P. O. Box 13-00044, Frascati, Italy; ¶Dipartimento Medicina Sperimentale, University L'Aquila, L'Aquila, Italy; and §Unitat de Biofísica, Departament de Bioquímica i de Biologia Molecular, Facultat de Medicina, Universitat Autònoma de Barcelona, Barcelona, Spain

ABSTRACT In this article we report x-ray absorption measurements of Ca^{2+}-substituted bacteriorhodopsin. We present a detailed study of the absorption spectrum close to the absorption edge that is very sensitive to the site geometry. We combined *ab initio* calculations of the x-ray absorption cross section based on a full multiple scattering approach, with a best fit of the experimental data performed by changing the cluster geometry. The Ca^{2+}-bacteriorhodopsin environment is composed of six oxygen atoms showing a distorted orthorhombic symmetry, whereas the Ca^{2+} in water solution has a regular octahydrated first sphere of coordination. Our results are in good agreement with previous molecular models suggesting that the high-affinity cationic site could be in the proximity of the retinal pocket. Our results provide strong direct evidence of the specific binding site of the metal cation in bacteriorhodopsin.

INTRODUCTION

Bacteriorhodopsin (BR) is a 26-kDa chromophoric transmembrane protein formed by seven transmembrane helices, connected by interhelical loops. It has a retinal molecule covalently linked to Lys-216 through a protonated Schiff base. When it absorbs a photon, it undergoes a photochemical cycle during which the retinal configuration changes from all-*trans* to 13-*cis*. This induces protein conformational changes that result in the translocation of a proton from the inside to the outside of the cell, returning both the retinal molecule and the protein to their initial states. In this way, bacteriorhodopsin converts the energy of light into an electrochemical proton gradient, which is used by the bacteria to produce ATP by ATP synthases.

Bacteriorhodopsin, which imparts the color of the purple membrane (PM) of *Halobacterium salinarum*, is synthesized under anaerobic conditions as an alternative way to obtain energy from light. Apart from bacteriorhodopsin (75% w/w) PM also contains phospho- and sulpholipids (25% w/w) (Dracheva et al., 1996). Native purple membrane contains divalent cations (~1 mol of Ca^{2+} and 4 mols of Mg^{2+} to 1 mol of BR) (Kimura et al., 1984; Chang et al., 1985), that are necessary to maintain the protein structure and its function. Removal of these cations from the PM by ion exchange or any other method increases the apparent pK of the blue/purple transition from ~3.2 in water to 5.5. Therefore, the proton pumping activity is stopped below pH 5.5 in the deionized membrane (Kimura et al., 1984; Chang et al., 1985; Duñach et al., 1987). This change is reversible by addition of a variety of mono-, di-, or trivalent cations (Kimura et al., 1984; Ariki and Lanyi, 1986; Duñach et al., 1987).

From a structural point of view, bacteriorhodopsin is probably one of the most extensively studied membrane proteins. In particular, the exact localization of the specific cation binding sites in bR is currently a matter of discussion and subject to numerous studies (Sepulcre et al., 1996; Eliash et al., 1999, 2001; Tuzi et al., 1999; Wang and El-Sayed, 2001; Sanz et al., 2001) because of its relevance in the relationship between the protein structure and its function.

The cation binding has been explained in terms of specific chemical binding to these negatively charged groups. Different affinity sites, five of high and medium affinity, and five of low affinity, have been found, although their localization is not yet clear (Duñach et al., 1987). For the high affinity binding site, an internal localization close to the retinal molecule has been proposed by several groups (Jonas and Ebrey, 1991; Zhang et al., 1992; Tan et al., 1996; Pardo et al., 1998), whereas for the medium- and low-affinity binding sites a surface localization near Glu-194 was suggested (Sanz et al., 2001), as well as a specific binding to the negatively charged lipids of the cellular membrane (Eliash et al., 2001). In contrast, another model suggested that the cation binding occurs nonspecifically at the membrane surface, via the Gouy-Chapman theory (Szundi and Stoeckenius, 1989).

In the last years, several three-dimensional models have been published, but so far, none of them gives any evidence about the cations' role or binding site, even the high-resolution x-ray diffraction experiments at 1.55 Å (Luecke et al., 1999, 2000; Belrhali et al., 1999). This is perhaps because the cations are partially or completely lost upon crystallization.

Submitted June 20, 2003, and accepted for publication March 8, 2004.

Address reprint requests to Dr. Francesc Sepulcre Sanchez, Universitat Politècnica de Catalunya, Enginyeria Agroalimentària i Biotecnologia, Urgell 187, Barcelona, 08036 Spain. Tel.: 34-93-4137410; E-mail: francesc.sepulcre@upc.es.

0006-3495/04/07/513/08 $2.00

doi: 10.1529/biophysj.103.030080

X-ray absorption spectroscopy (XAS) can provide direct information about the local structure of the cation, allowing study of the purple membrane in suspension, i.e., in an environment that is close to its real physiological state. It also has the advantage of being element-specific and not requiring a crystalline sample. Such studies on Mn^{2+}-substituted BR are reported in our previous work (Sepulcre et al., 1996); they provide evidence for octahedral coordination of Mn^{2+} with six oxygen atoms located in the protein molecule.

In this work we report x-ray absorption measurements of Ca^{2+}-substituted bacteriorhodopsin. The x-ray absorption spectra are usually split into two different regions, an extended region (EXAFS) ranging from ~40 to 1000 eV above the absorption edge, and a near-edge region (XANES), including the absorption edge and 50–100 eV above it (Benfatto et al., 1986; Tyson et al., 1992). In the EXAFS region the photoelectron scattering is mostly determined by single scattering mechanisms, and a quite simplified analysis of the fine structure oscillations can easily give valuable structural information as the average near-neighbor distances, coordination number, and type of neighbor atom around the absorbing cation. The XANES region is instead sensitive both to the electronic structure of the absorbing atom and to the geometrical structure of the scatterers. The interpretation of the XANES spectrum is more complex than EXAFS; it requires more complicated ab initio calculations of the scattering cross section taking into account multiple scattering events that are dominant at low photoelectron energies. On the other side its information content is particularly rich. In our case, for example, it allows us to determine bond angles and geometry coordination together with interatomic distances of the Ca^{2+} cluster, which are important in determining the nature of the Ca^{2+} binding site.

In the following we report the results of the geometrical fitting of the XANES region of Ca^{2+}-substituted BR. In order to search the local environment of the high-affinity binding site of Ca^{2+} in PM we have measured the x-ray absorption spectra of deionized blue membrane regenerated with 1 Ca^{2+} per mol of BR. At this calcium concentration only the high-affinity binding site of BR should be filled. The results are discussed in terms of proposed models for the metal cation binding site in the protein. The detailed XANES analysis of the Ca^{2+}-BR complex and of Ca^{2+} in water based on the full multiscattering procedure MXAN (Benfatto and Della Longa, 2001) shows differences in the coordination number as well as in the geometry of the next nearest neighbors.

MATERIALS AND METHODS

Purple membrane was isolated from the *Halobacterium salinarum* strain S9 as described previously (Oesterhelt and Stoeckenius, 1974). Cations were removed from purple membrane suspensions by dialysis for 6 h against a Dowex AG-50 W cation exchange resin. A separated aliquot of deionized membrane was always used for pH and spectroscopic controls to avoid any possibility of contamination. Regeneration was done at pH 5 by adding Ca^{2+} at a molar ratio of 1:1 (Ca^{2+}/BR) and checked by ultraviolet spectroscopy, verifying that the absorption band shifts, as expected, from 600 nm to 580–590 nm.

Measurements of the calcium K-edge were carried out at the beam line ID26 of the European Synchrotron Radiation Facility that is dedicated to the study of very diluted systems, requiring high photon flux ($>10^{13}$ ph/s). Monochromatic beam was obtained by means of a Si[111] double crystal monochromator, with an energy resolution $\Delta E/E = 1.4 \times 10^{-4}$. Vertical and horizontal focusing of the incident beam was achieved by means of Pt-coated silica mirrors, also providing harmonic rejection of high energy photons. The samples were deposited on the sample holders and were kept overnight in a close chamber to get a partially dried film by applying a mild vacuum. The fluorescence signal at the Ca K-edge, was detected by a multielement silicon-drift solid state detector. The absorption spectrum of Ca^{2+} in water, at a concentration of 50 mM, was also recorded as a reference system. Measurements at the Ca K-edge were carried out at room temperature. In order to minimize the sample exposure to radiation we used a quick scan method developed at ID26, consisting of data acquisition during a continuous energy scan of the crystal monochromator. The individual energy scans lasted ~1 min. The sample was moved automatically every five scans and the results we show correspond to an average over ~12 h.

The MXAN for simulation and XANES fitting code

In order to extract the structural/geometrical information on the Ca^{2+} first coordination shell that is contained in the fine structure just above the edge, we performed a quantitative analysis of the XANES spectrum using the MXAN code. This method is based on the comparison between experimental data and many theoretical calculations performed by varying selected structural parameters starting from a putative structure, i.e., from a well-defined initial geometrical configuration around the absorber. The calculation of XANES spectra related to the hundreds of different geometrical configurations needed to obtain the best fit of the experimental data is done in the framework of the full multiple-scattering calculation, i.e., the scattering path operator $\boldsymbol{\tau}$ is calculated exactly, and the optimization in the space of parameters is achieved by the minimization of the square residual function in the parameter space. In this way the low energy part of the XAS spectrum is completely available for a quantitative analysis and we can benefit for the extreme sensitivity of this energy region to the structural details of the absorbing site (overall symmetry, distances, and bond angles).

The MXAN method is based on the muffin-tin approximation for the shape of the potential and uses the concept of the complex optical potential to account for the inelastic losses of the photoelectron in the final state. To avoid the overdamping at low energies of the complex part of the HL potential in the case of covalent molecular systems, we use here a phenomenological treatment of the inelastic losses based on a convolution with a broadening Lorentzian function having an energy-dependent width of the form $\Gamma(E) = \Gamma_c + \Gamma_{mfp}(E)$. The constant part Γ_c includes the core-hole lifetime and the experimental resolution, whereas the energy-dependent term represents all the intrinsic and extrinsic inelastic processes. The $\Gamma_{mfp}(E)$ function is zero below an onset energy E_s (which in extended systems corresponds to the plasmon excitation energy) and begins to increase from a value A_s following the universal functional form of the mean free path in solids. Both, the onset energy E_s and the jump A_s, are introduced in the $\Gamma_{mfp}(E)$ function via an arctangent functional form to avoid discontinuities. Both numbers are derived via a Monte Carlo fit at each step of the computation (i.e., for each geometrical configuration) using a procedure similar to that in the simulated annealing method (Kirkpatrick et al., 1983). This type of approach is justified by the equivalence of the use of a suitable complex self-energy in the calculation and a convolution of the photoabsorption cross section, calculated with the real part of the self-energy, with a Lorentzian function with a well-defined energy-dependent width. The

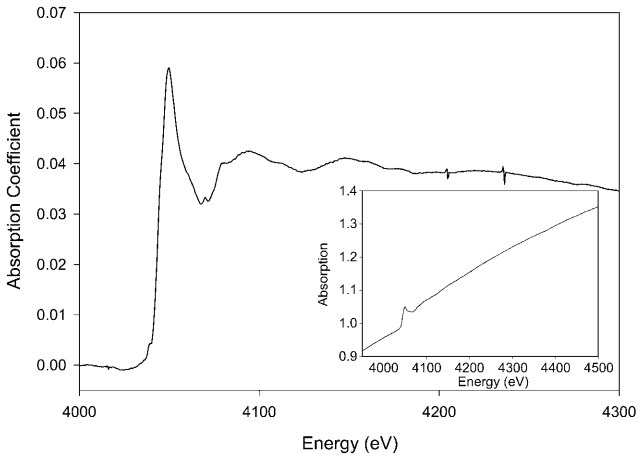

FIGURE 1 Calcium K-edge absorption spectra of well-washed PM. (*Inset*) X-ray absorption signal before background subtraction.

application of this method has given very good results for different systems as, for example, metal-water complexes and potassium ferrocyanide. We refer the interested reader to a series of very recent articles. (Benfatto and Della Longa, 2001; Della Longa et al., 2001, 2003; Benfatto et al., 2002a, 2000b; D'Angelo et al., 2002; Hayakawa et al., in 2003).

In the case of test systems the right geometrical configuration has been recovered, starting from a distorted geometry, within an error of the order of 2–4 degrees in the angle determination and 0.02 Å in the interatomic distances. Moreover, the geometrical determination at the fitted condition shows to be very stable with respect to the changes of some nonstructural parameters, as the muffin-tin radii, confirming the dominance of the geometrical arrangements over the electronic configurations in the construction of the photoabsorbing cross section.

RESULTS

Fig. 1 displays the raw absorption spectra corresponding to a well-washed purple membrane (six to seven washes with distilled water). Although the absorption signal is too weak to perform a quantitative XANES analysis, it is indicative of the presence of some Ca^{2+} atoms tightly bound, as expected if this cation is located in a cluster with a specific geometry (i.e., a high- and/or medium-affinity binding site). Otherwise, the successive washes should shift the equilibrium completely to the Ca^{2+}-water form.

The XANES spectra of deionized PM after reconstitution with Ca^{2+} at a molar ratio of 1:1 (Ca^{2+}/BR) and of a Ca^{2+}-water solution are shown as solid lines in Fig. 2, *A* and *B*, respectively. The experimental spectra of both the Ca^{2+}-BR complex and Ca^{2+} in water show a small shoulder at ~40 eV above the edge due, probably, to a multiple excitation.

Ca^{2+} cluster modeling

The MXAN program performs an *ab initio* calculation of the XANES spectrum for a reference cluster, allowing a refinement both of its structural parameters, such as bond lengths and bond angles, and nonstructural parameters, such as Γ_c and the energy onset and jump intensity of Γ_{mfp}, which are defined in the previous section. Therefore we have chosen some possible model clusters as a starting point and refined them to obtain the best fit to the experimental spectrum. The best-fit model showing the best agreement with the experiment is the one giving the least normalized residual value.

Carboxyl side chains of Asp and Glu residues have been proposed as candidates for cation binding in BR (Jonas and Ebrey, 1991; Stuart et al., 1995; Yang and El-Sayed, 1995; Wang and El-Sayed, 2001; Sanz et al., 2001). On the other hand, all the three-dimensional models of bacteriorhodopsin show different Asp and Glu groups that in terms of geometry and bond lengths are compatible with cation binding sites (Luecke et al., 1999, 2000; Belrhali et al., 1999). Therefore, as a starting point of the theoretical calculations, it is reasonable to consider as putative structures for both the protein and water different clusters in which the first coordination shell (nearest neighbor) is formed by oxygen atoms. On the basis of this assumption, we have considered five different geometrical starting models for the nearest-neighbor shell (labeled from S6 to S9):

1. S6, Ca-6O (orthorhombic, Ca-O at 2.33 Å).
2. S7, Ca-7O (capped trigonal prism, Ca-O at 2.40 Å).
3. S8r and S8a, Ca-8O (regular square and antiregular square, respectively, Ca-O at 2.48 Å).
4. S9, Ca-9O (tricapped trigonal prism, Ca-O at 2.53 Å).

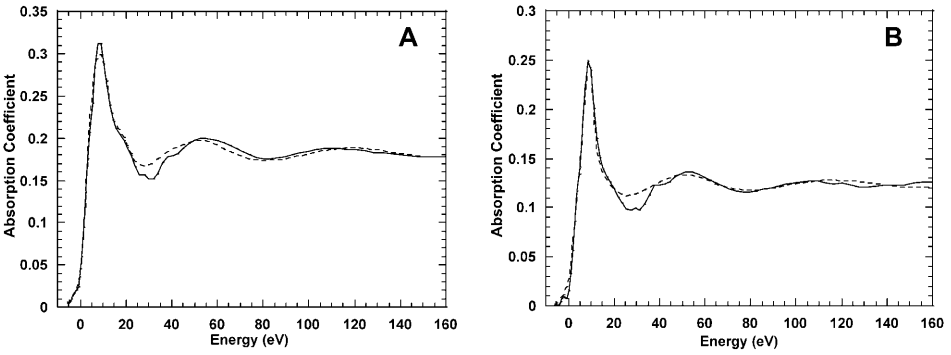

FIGURE 2 Theory-versus-experiment best-fit results for Ca^{2+}-BR complex starting from cluster S6 (*A*), and for Ca^{2+} in water starting from cluster S8r (*B*). All the Ca-O distances are considered as independent parameters.

TABLE 1 Best fit results for the Ca^{2+}-BR complex and for Ca^{2+} in water

Starting structure	Res.	$\langle r_{Ca\text{-}O} \rangle$ (Å)	Γ_c (eV)
Ca^{2+}-BR complex			
S6	4.25	2.32	1.18
S7	5.54	2.32	1.22
S8r	4.42	2.29	1.02
S8a	6.57	2.32	1.22
Ca^{2+} in water			
S6	7.22	2.37	1.00
S7	5.40	2.34	1.10
S8r	4.34	2.36	1.14
S8a	4.95	2.36	1.17

The Ca-O distances reported are the average of the values found considering all the Ca-O distances in the clusters as independent parameters (see text). Γ_c is the energy-independent broadening factor.

We used two different approaches in refining the interatomic distances of the starting cluster:

a. We started the calculations considering all the Ca-O distances as independent parameters and letting them vary simultaneously. The fitting results are presented in Table 1 for BR and Ca^{2+}-water solution, respectively. The best fit for the Ca^{2+}-BR spectrum was obtained for the starting geometrical configuration S6, corresponding to a distorted first shell formed by six oxygen atoms at a mean Ca-O distance of 2.32 Å, with a value of the normalized square residual function S^2/n of 4.25. The comparison between the experimental absorption data of the Ca^{2+}-BR complex and the best fit is shown in Fig. 2 *A*, in which a good agreement between both curves is apparent. The best-fit curve for Ca^{2+} in water, obtained using the same starting atomic clusters as for the protein sample, is shown in Fig. 2 *B*. In this case the best fit is attained by a different cluster, S8r, and the refined structure corresponds to a regular square for the first hydration shell ($n = 8$) of the calcium atom at an average distance of 2.36 Å. Table 1 also shows the best-fit values for the nonstructural parameter Γ_c. As can be observed, we always find values of ~1 eV that are in reasonable agreement with the convolution of the theoretical core-hole value of ~0.8 eV for Ca with the expected experimental resolution of ~0.4 eV.

b. A second group of calculations was performed introducing some constraints in the possible displacements of the oxygen atoms with respect to the starting symmetrical positions. Thus, the opposite oxygen atoms with respect to the Ca^{2+} were forced to move together during the fitting process (i.e., the Ca^{2+}-O distances corresponding to the opposite atoms change simultaneously) and were considered as a single parameter. This constraint slightly optimizes the agreement between theory and experiment compared to the previous calculations. The results are shown in Fig. 3 for the Ca^{2+}-BR complex (*A*) and the Ca^{2+}-water solution (*B*). For the Ca^{2+}-BR complex, the best fit ($S^2/n = 4.17$) corresponds again to a distorted square cluster of six oxygen atoms around the metal cation at a mean distance of 2.31 Å and it was obtained starting from the same S6 structure. For the Ca^{2+}-water sample, the best fit ($S^2/n = 3.99$) was obtained for a regular square configuration around the Ca ion at an average distance of 2.35 Å, corresponding to the same starting cluster S8r as in the previous case.

A view of the corresponding clusters is shown in Fig. 4. As can be observed, the Ca^{2+} bound to the protein has a regular octahedral coordination shell formed by six oxygen atoms at a mean distance of 2.31 Å (Fig. 4 *A*), whereas the structure of Ca^{2+} in water displays a square geometry (octahydrated calcium ion), with the mean distance Ca-O of 2.35 Å (Fig. 4 *B*). Although the average interatomic distances for the Ca^{2+}-protein and the Ca^{2+}-water are not very different, the cluster geometry is not at all the same. Table 2 shows the individual Ca-O distances, corresponding to best fits, for BR and Ca^{2+}-water solution. Statistical errors on distance values have been evaluated by the least-squares minimization routine from correlation matrix, and they are in all cases <0.01 Å. The values found for the solution sample show, indeed, quite a wide spreading, corresponding, actually, to a distorted square geometry.

A Ca^{2+} protein binding site

Several studies have suggested that a divalent cation is located in the proximity of the retinal binding pocket (Jonas and

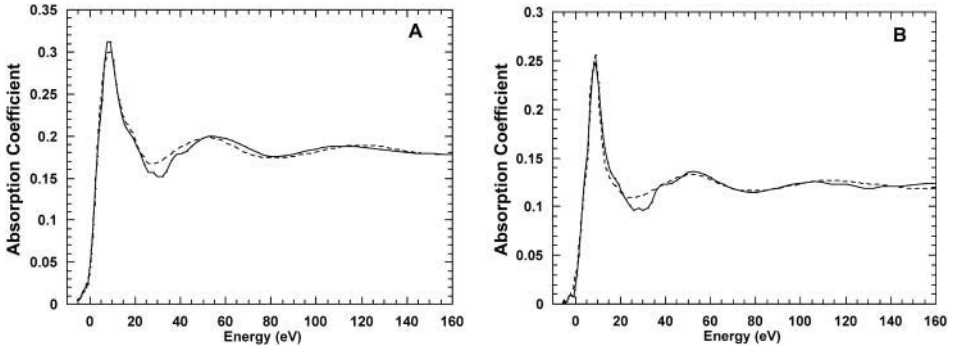

FIGURE 3 Theory-versus-experiment best-fit results for Ca^{2+}-BR complex starting from cluster S6 (*A*) and for Ca^{2+} in water starting from cluster S8r (*B*). All the Ca-O distances are correlated.

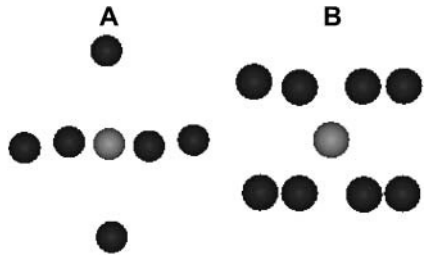

FIGURE 4 Ca^{2+} clusters corresponding to the best-fit results shown in Fig. 2 *A* (*A*) and Fig. 2 *B* (*B*).

Ebrey, 1991; Zhang et al., 1992; Tan et al., 1996; Pardo et al., 1998) associated with Asp-85 and Asp-212. It should belong to a cluster formed by Asp-212, Asp-85, and three water molecules (as described in Pardo et al., 1998) leading to similar characteristics, in terms of coordination number (6) and geometry, as our model S6 for the first Ca coordination shell which shows the best agreement with the experimental XANES data. This suggests, therefore, that this BR internal cluster can be a cation binding site.

To verify this hypothesis, we performed a fitting of the experimental data with a molecular model obtained from the optimized geometry of Pardo et al., (1998) by selecting a sphere with a radius of 6 Å centered on the absorbing atom containing the side chains of Asp-85 and Asp-212, three water molecules, and a part of the retinal chromophore. The starting cluster to be refined includes six oxygen atoms in a distorted octahedral-like configuration with the Ca-O distances varying from 1.98 Å to 2.24 Å, corresponding to an average distance of 2.12 Å. No hydrogen atoms have been included in the calculation. The results of this analysis are shown in Fig. 5 and Table 3. The best fit of the experimental data, showing a S^2/n value of 1.79, corresponds to a first coordination shell of 6 O atoms with a Ca-O average distance of 2.31 Å. Therefore, the refinement results in an increase of the average Ca-O distance, as expected from the increased ionic radius of Ca^{2+} in comparison with the Mg cation of the model (Pardo et al., 1998). On the other hand, the Ca-O distances in the refined cluster vary from 2.22 Å to 2.37 Å,

TABLE 2 Individual Ca-O distances corresponding to the best-fit models for the Ca^{2+}-BR complex and Ca^{2+} in water

BR-S6	Ca^{2+}sol.-S8r
$r_{Ca\text{-}O}$ (Å)	$r_{Ca\text{-}O}$ (Å)
2.32	2.31
2.32	2.40
2.32	2.33
2.32	2.37
2.32	2.31
2.32	2.31
	2.52
	2.31

All Ca-O values in the clusters are considered as independent parameters (see text). The statistical error in all cases is <0.01 Å.

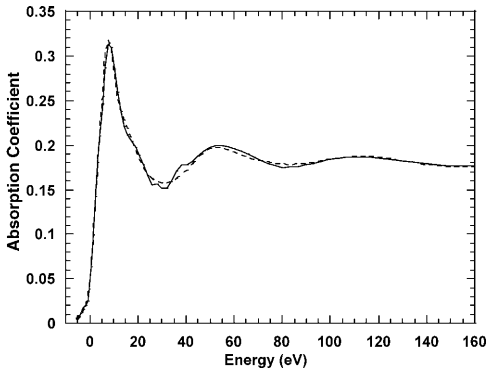

FIGURE 5 Theory-versus-experiment best-fit results for Ca^{2+}-BR complex starting from Asp-85-Asp-212-3 H_2O cluster.

i.e., the distance spread appears to be reduced with respect to the starting cluster. The agreement between the experimental data and the fitting calculations is very good, even better than that for model S6, clearly suggesting that this internal cluster formed by Asp-85, Asp-212, and three water molecules is a possible high-affinity binding site in the protein. Fig. 6 shows a detailed view of the computed Asp-85-Asp-212-3 H_2O cluster for the best fit. As can be observed, the first sphere around the Ca^{2+} ion has a very distorted octahedral coordination formed by the O atoms of Asp-212, the O1 atom of Asp-85, and three water molecules. The Ca-O bond lengths and the angles between the water molecules, W1, W2, and W3, are reported in Tables 3 and 4. The angles are compared with those reported in recent studies on crystallized BR (Belrhali et al., 1999; Luecke et al., 1999, 2000).

DISCUSSION

In this article we present a quantitative analysis of the XANES spectrum of Ca^{2+}-regenerated bacteriorhodopsin to characterize geometrically the high-affinity binding site. The study of the XANES spectra gives information on the geometrical structure of the absorbing atom site as, for example, distances, symmetry, and angles. This kind of analysis is particularly important in cases like this, where the limited *k*-range of experimental data makes it difficult to use the EXAFS spectra. This analysis is based on the assumption that the first coordination shell of the high-affinity binding site of the purple membrane is formed by oxygen atoms. On

TABLE 3 Best fit Ca-O distances and angles for the Ca^{2+}-BR complex, obtained starting from the molecular dynamics model by Pardo et al. (1998) made by an Asp-85-Asp-212-3 H_2O cluster

	Asp-85-Asp-212-3 H_2O						
	Asp-85		Asp-212				
Group	O1	O2	O1	O2	W1	W2	W3
$r_{Ca\text{-}O}$ (Å)	2.31	3.36	2.22	2.37	2.25	2.36	2.29

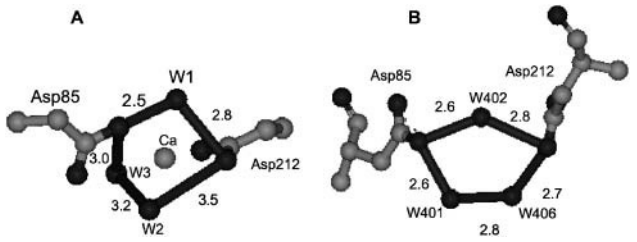

FIGURE 6 Ca^{2+} coordination in the vicinity of the Schiff base, corresponding to the best-fit for the Ca^{2+}-BR complex, starting from the putative cluster described in the reference by Pardo et al. (1998).

the other hand, calcium ions are known to bind strongly phosphate groups, but the EXAFS part of our data (data not shown) does not support the presence of phosphorus or sulfur atoms in the second shell because no significant contribution beyond the first peak of the Fourier transform is observed. Therefore, we assume that the Ca^{2+} binding site is located in the protein, in full agreement with a previous work indicating that the high-affinity Mn^{2+} binding site is also located in the protein (Sepulcre et al., 1996). In the framework of this hypothesis, we have performed a theoretical test on the Ca^{2+} K-edge of several coordinations (from 6 to 9) and geometries to compare them with the experimental data. In this way, we take advantage of the high sensitivity of the XANES spectrum on the local coordination chemistry of the absorbing atom.

It should be noted that the determination of the identity and geometry of the first nearest neighbors represents a notoriously difficult problem because of the flexibility of the first coordination sphere and the low atomic number of the atoms involved. Our results can also be compared with more recent results (Fulton et al., 2003) in which a distance of 2.43 ± 0.01 Å is found by EXAFS of Ca^{2+} aqueous solution. This makes a difference of 0.07 Å with respect to our finding of 2.36 Å. It has to be noted that in Fulton's study, the coordination number found is 7, with a quite large error of ±1.2. The distance value we find for a coordination number, $N = 7$, is 2.34 ± 0.07 Å, that is, very close, within the experimental error, to Fulton's value. These large errors on coordination numbers found by EXAFS could also be ascribed to the wide spread in the interatomic distances (that is probably associated to the complex configurational changes that this kind of system can undergo). We have no news of any other study that takes this into account, as we do, by fitting all the oxygen distances as independent parameters. Moreover, we must mention that we have detected a slight systematic shrinking of interatomic-distance absolute values of 0.02–0.03 Å, in the MXAN simulation. This is due to the Hedin -Lundqvist potential behavior, which is nearly constant for the first 30–40 eV after the edge. This effect is discussed in detail in the article by D'Angelo et al. (2002). This could shift our value of 2.36 to 2.39 Å, that is, even less far from the previous EXAFS determination. Moreover, this would be in full agreement with a recent, yet unpublished study by P. D'Angelo (2004, private communication), in which a value of 2.39 Å is found for the Ca-O distance in aqueous solution.

A coordination number of 8 for Ca^{2+} ion in water was also proposed by Albright (1972) in his x-ray diffraction study of aqueous $CaCl_2$ solution. XAS studies on several Ca complexes such as Ca-formate, Ca-glutamate, and Ca-EGTA (Alemà et al., 1982; Einspahr and Bugg, 1977) have shown that the intensity of the resonance at ~20 eV above the edge increases as the coordination number of the metal atom decreases. Our results are in agreement with this observation: the complex Ca^{2+}-BR, which shows a stronger peak intensity at 20 eV than the complex Ca^{2+}-water, has a coordination number of 6, whereas the Ca^{2+} in water has a coordination number of 8 (see Fig. 3).

Einspahr and Bugg (1977) reported common features about the geometry of the Ca-carboxyl interaction by studying 60 crystal structures containing Ca. In particular they found that 1), bidentate-chelated calcium ions are confined to a restricted range of interactions with both oxygen atoms of the carboxyl group, posessing C-O-Ca angles of ~90°; 2), the unidentate and bidentate interactions display an average Ca-O distance of ~2.37 Å and 2.54 Å, respectively and; 3), the average distance for Ca contacts with carboxyl-oxygen atoms are ~2.35 Å for sixfold coordination. The results described in the present work are in reasonable agreement with these features. First, the C-O-Ca angles in the Ca-Asp-212 carboxyl bidentate interactions are both very close to 90° (86.16° and 89.75°). Second, the Ca-O distance in the unidentate Ca-Asp-85 carboxyl interaction is 2.31 Å (see Table 3) in comparison with 2.37 Å found by Einspahr and Bugg. Third, the Ca-O average distance found by us (2.30 Å) agrees well with the value proposed for sixfold coordination by those authors (2.35 Å).

From our results, it is clear that the first coordination shell for the metal atom is different when it is bound to the protein

TABLE 4 Best-fit angles between the three water molecules W1, W2, and W3, of model by Pardo et al. (1998), and the three water molecules, W401, W402, and W406, belonging to the cluster labeled 1C3W of the model proposed by Luecke et al. (1999)

Model			
1C3W	W402-W401-W406	W401-W406-W402	W401-W402-W406
	69.9°	64.0°	46.1°
Asp-85-Asp-212-3W	W1-W3-W2	W3-W2-W1	W3-W1-W2
	72.1°	61.6°	46.3°

or is solvated by water molecules. When the calcium ion is in the presence of the protein, its first coordination shell is composed of six oxygen atoms showing a distorted orthorombic symmetry, whereas if the metal is in water solution, it has a very regular octahydrated first sphere of coordination. These results imply that the calcium tends to interact with the protein rather than with the water. Such a significant difference between the Ca^{2+} environments establishes that the high-affinity binding site has to be internal to the protein, otherwise it would be hydrated (i.e., showing a XANES signal similar to Ca^{2+} in water). These results are consistent with our previous EXAFS work in which we found an octahedral geometry for the high-affinity Mn^{2+} binding site (Sepulcre et al., 1996). This similarity suggests that both cations (Mn^{2+} and Ca^{2+}) bind to the same high-affinity binding site.

A further confirmation of our model goodness is also given by previous articles (Belrhali et al., 1999; Luecke et al., 1999, 2000) on the crystallographic structure of bacteriorhodopsin, which report about the presence of internal water molecules near the Schiff base region, forming a pentagonal cluster. Such a kind of cluster is well visible indeed in our model shown in Fig. 6. Again, our results are consistent with a location of the high-affinity cation binding site in the retinal pocket. This does not exclude the possibility of a further binding site, in the extracellular region, in the cluster formed by Glu-194, Glu-204 groups, and the water molecules close to them, as suggested by previous studies (Sanz et al., 2001). In any case, our results are a strong evidence of the specific binding site of the metal cation to bacteriorhodopsin. An additional issue is why any of the crystallographic structures does not show bound cations. One reason could be that due to the methods used in the crystal preparation the native cations are lost and substituted by monovalent cations, which, having a higher mobility around the binding site(s), are not detectable by crystallographic methods.

The authors gratefully acknowledge Beamline ID26 of European Synchrotron Radiation Facility for granting in-house research beamtime, and in particular Dr. A. Sole for his kind technical assistance and fruitful discussions during the experiments.

M.G.P. and M.B. acknowledge the support of the INFN-CICYT collaboration agreement 2002-2003.

This work was in part supported by the Dirección General de Investigación, MCYT (grant BMC2000-0121) and the Dirección General de Recerca, DURSI (grant 2001SGR-197).

REFERENCES

Albright, J. 1972. X-ray diffraction studies of aqueous alkaline-earth chloride solutions. *J. Chem. Phys.* 56:3783–3786.

Alemà, S., A. Bianconi, L. Castellani, and P. Fasella. 1982. X-ray absorption spectroscopy (EXAFS and XANES) a structural tool for calcium binding proteins: effect of Mg^{2+} on Ca^{2+} binding sites of troponin-C. *Prog. Clin. Biol. Res. C.* 102:47–57.

Ariki, M., and J. K. Lanyi. 1986. Characterization of metal ion-binding sites in bacteriorhodopsin. *J. Biol. Chem.* 261:8167–8174.

Belrhali, H., P. Nollert, A. Royant, C. Menzel, J. P. Rosenbusch, E. M. Landau, and E. Pabay-Peyroula. 1999. Protein, lipid and water organization in bacteriorhodopsin crystals: a molecular view of the purple membrane at 1.9 Å resolution. *Structure*. 7:909–917.

Benfatto, M., P. D'Angelo, S. Della Longa, and N. V. Pavel. 2002a. Evidence of distorted fivefold coordination of the Cu^{2+} aqua ion from an X-ray absorption spectroscopy quantitative analysis. *Phys. Rev. B.* 65: 174205-1–174205-5.

Benfatto, M., J. A. Solera, J. García Ruiz, and J. Chaboy. 2002b. Double-channel excitation in the X-ray absorption spectrum of Fe^{3+} water solutions. *Chem. Phys.* 282:441–450.

Benfatto, M., and S. Della Longa. 2001. Geometrical fitting of experimental XANES spectra by a full multiple-scattering procedure. *J. Synchrotron Rad.* 8:1087–1094.

Benfatto, M., C. R. Natoli, A. Bianconi, J. Garcia, A. Marcelli, M. Fanfoni, and I. Davoli. 1986. Multiple scattering regime and higher-order correlations in x-ray absorption spectra of liquid solution. *Phys. Rev. B.* 34:5774–5781.

Chang, C. H., J.-G. Chen, R. Govindjee, and T. Ebrey. 1985. Cation binding by bacteriorhodopsin. *Proc. Natl. Acad. Sci. USA.* 82:396–400.

Cladera, J., M. L. Galisteo, M. Duñach, P. L. Mateo, and E. Padrós. 1988. Thermal denaturation of deionized and native purple membranes. *Biochim. Biophys. Acta.* 943:148–156.

D'Angelo, P., M. Benfatto, S. Della Longa, and N. V. Pavel. 2002. Combined XANES and EXAFS analysis of Co^{2+}, Ni^{2+}, and Zn^{2+} aqueous solutions. *Phys. Rev. B.* 66:064209-1–064209-7.

Della Longa, S., A. Arcovito, M. Girasole, J. L. Hazemann, and M. Benfatto. 2001. Quantitative analysis of the x-ray absorption near edge structure data by a full multiple scattering procedure: the Fe-Co geometry in photolyzed carbonmonoxy-myoglobin single crystal. *Phys. Rev. Lett.* 87:155501-1–1555501-4.

Della Longa, S., A. Arcovito, M. Benfatto, A. Congiu-Castellano, M. Girasole, J. L. Hazemann, and A. Lo Bosco. 2003. Redox-Induced Structural Dynamics of Fe-Heme ligand in Myoglobin by X-ray absorption spectroscopy. *Biophys. J.* 85:549–558.

Dracheva, S., S. Bose, and R. W. Hendler. 1996. Chemical and functional studies on the importance of purple membrane lipids in bacteriorhodopsin photocycle behavior. *FEBS Lett.* 382:209–212.

Duñach, M., M. Seigneuret, J. L. Rigaud, and E. Padrós. 1987. Characterization of the cation binding sites of the purple membrane. Electron spin resonance and flash photolysis studies. *Biochemistry.* 26:1179–1186.

Einspahr, H., and C. E. Bugg. 1977. Cristal structures of calcium complexes of amino acids, peptides and related model systems. *In* Calcium Binding Proteins and Calcium Function. R. H. Wasserman, R. A. Corradino, E. Carafoli, R. H. Kretsinger, D. H. MacLennan, and F. L. Siegel, editors. Elsevier North-Holland, Amsterdam. 13–20.

Eliash, T., M. Ottolenghi, and M. Sheves. 1999. The titration of Asp-85 and of the cation binding residues in bacteriorhodopsin are not coupled. *FEBS Lett.* 447:307–310.

Eliash, T., L. Weiner, M. Ottolenghi, and M. Sheves. 2001. Specific binding sites for cations in bacteriorhodopsin. *Biophys. J.* 81:1163–1170.

Fulton, J. L., S. M. Heald, Y. S. Badyal, and J. M. Simonson. 2003. Understanding the effects of concentration on the solvation structure of Ca^{2+} in aqueous solution. I. The perspective on local structure from EXAFS and XANES. *J. Phys. Chem. A.* 107:4688–4696.

Hayakawa, K., K. Hatada, C. R. Natoli, P. D'Angelo, and M. Benfatto. 2003. A quantitative structural investigation of the XAS spectra of potassium ferrocyanide (II,III) at the Fe K-edge. *Proc. EXAFS XII Conf. Malmö. Phys. Scripta.* In press.

Jonas, R., and T. G. Ebrey. 1991. Binding of a single divalent cation directly correlates with the blue-to-purple transition in bacteriorhodopsin. *Proc. Natl. Acad. Sci. USA.* 88:149–153.

Kimura, Y., A. Ikegami, and W. Stoeckenius. 1984. Salt and pH-dependent changes of the purple membrane absorption spectrum. *Photochem. Photobiol.* 40:641–646.

Kirkpatrick, S., C. D. Gelatt, and M. P. Vecchi. 1983. Optimization by simulated annealing. *Science*. 220:671–680.

Luecke, H., B. Schobert, J. P. Cartailler, H. T. Richter, A. Rosengarth, R. Needleman, and J. K. Lanyi. 2000. Coupling photoisomerization of retinal to directional transport in bacteriorhodopsin. *J. Mol. Biol.* 300:1237–1255.

Luecke, H., B. Schobert, H. T. Richter, J. P. Cartailler, and J. K. Lanyi. 1999. Structure of bacteriorhiodopsin at 1.55 Angstrom resolution. *J. Mol. Biol.* 291:899–911.

Oesterhelt, D., and W. Stoeckenius. 1974. Isolation of the cell membrane of Halobacterium halobium and its fractionation into red and purple membrane. *Methods Enzymol.* 31:667–678.

Pardo, L., F. Sepulcre, J. Cladera, M. Duñach, A. Labarta, J. Tejada, and E. Padrós. 1998. Experimental and theoretical characterization of the high-affinity cation-binding site of the purple membrane. *Biophys. J.* 75: 777–784.

Sanz, C., M. Marquez, A. Perálvarez, S. Elouatik, F. Sepulcre, E. Querol, T. Lazarova, and E. Padrós. 2001. Contribution of extracellular Glu residues to the structure and function of bacteriorhodopsin. *J. Biol. Chem.* 276:40788–40794.

Sepulcre, F., J. Cladera, J. García, M. G. Proietti, J. Torres, and E. Padrós. 1996. An extended x-ray absorption fine structure study of the high-affinity cation-binding site in the purple membrane. *Biophys. J.* 70: 852–856.

Stuart, J. A., B. W. Vought, C. Zhang, and R. R. Birge. 1995. The active site of bacteriorhodopsin. Two-photon spectroscopic evidence for a positively charged chromophore binding site mediated by calcium. *Biospectroscopy*. 1:9–28.

Szundi, I., and W. Stoeckenius. 1989. Surface pH controls purple-to-blue transition of bacteriorhodopsin. A theoretical model of purple membrane surface. *Biophys. J.* 56:369–383.

Tan, E. H. L., D. S. K. Govender, and R. R. Birge. 1996. Large organic cations can replace Mg^{2+} and Ca^{2+} ions in bacteriorhodopsin and maintain proton pumping ability. *J. Am. Chem. Soc.* 118:2752–2753.

Tuzi, S., S. Yamaguchi, M. Tanio, H. Konishi, S. Inoue, A. Naito, R. Needleman, J. K. Lanyi, and H. Saito. 1999. Location of cation binding site in the loop between helices F and G of bacteriorhodopsin, as studied by ^{13}C-NMR. *Biophys. J.* 76:1523–1531.

Tyson, T. A., K. O. Hodgson, C. R. Natoli, and M. Benfatto. 1992. General multiple scattering scheme for the computation and the interpretation of x-ray absorption fine structure in atomic cluster with application to SF6, $GeCl_4$ and Br_2 molecules. *Phys. Rev. B*. 46:5997–6019.

Wang, J., and M. A. El-Sayed. 2001. The effect of metal cations binding on the protein, lipid and retinal isomeric ratio in regenerated bacteriorhodopsin of purple membrane. *Photochem. Photobiol.* 73:564–571.

Yang, D., and M. A. El-Sayed. 1995. The Ca^{2+} binding to deionized monomerized and to retinal removed bacteriorhodopsin. *Biophys. J.* 69:2056–2059.

Zhang, Y. N., L. L. Sweetman, E. S. Awad, and A. El-Sayed. 1992. Nature of the individual Ca^{2+} binding sites in Ca^{2+}-regenerated bacteriorhodopsin. *Biophys. J.* 61:1201–1206.